UDC 544.72+544.6.018+544.65+537.211+538.956

IMAGE FORCES IN PHYSICS AND CHEMISTRY OF SURFACES: CERTAIN FUNDAMENTAL ASPECTS

A.M. Gabovich

Institute of Physics of the National Academy of Sciences of Ukraine, 46, Nauka Avenue, Kyiv 03680, Ukraine

The occurrence and role of image forces in physics and chemistry of surfaces are analyzed. It is shown that a prima facie simple concept of classical electrostatics has a very complicated background of diverse many-body phenomena. In particular, attention is focused on dynamic effects usually small but, nevertheless, important due to their peculiar manifestations.

INTRODUCTION

One can conceive many cases when a charged particle is at rest or moving in an inhomogeneous structure near an interface (interfaces) between constituent media. Since dielectric functions $\varepsilon_i(\mathbf{q},\omega)$ of different media are, generally speaking, not identical, *additional polarization* of the interface regions emerges caused by the Coulomb field of the charge in question. Arguments $\mathbf{q}$ and ω are transferred wave vector (in this context we shall make no distinction between momenta and wave vectors by tacitly assuming the Planck's constant $\hbar$ equal to unity) and frequency, so that the polarization properties of any medium involved are considered non-local and retarded (i. e. non-local in time). In other words, introducing expressions $\varepsilon_i(\mathbf{q},\omega)$ we take into account spatial and temporal dispersions of the bulk polarizations [1–4]. Therefore, $\varepsilon(\mathbf{q},\omega)$ is a straightforward generalization of the conventional dielectric constant ε of the classical electrostatics [5].

An extra position- and time-dependent energy generated by the field of an extra charged particle near an interface is called *image force energy W*, and the corresponding forces are called *image forces*, the term being familiar to everybody who has ever read standard textbooks. In particular, the origin of the term goes back to electrostatics of conductors where a point charge *Ze* located near an ideal infinite neutral conductor at a distance $-z$ interacts with the metal surface in such a way as if an opposite charge $(-Ze)$ is positioned inside the metal at a distance (z) whereas the metal itself is not taken into account [6]

$$W(z) = -\frac{(Ze)^2}{4z}. \qquad (1)$$

Hereafter, we shall define *e* as a positive elementary charge, appropriate, say, to a proton. The number *Z* is an integer.

In the simplest approximations *W* near a metal surface is always attractive (< 0) as in Eq. (1), although the situation is much more complex in realistic approaches, better describing the experimental data and being more consistent from theoretical viewpoint. The subscript "*i*" in formulae for dielectric functions numbers the media.

It is necessary to emphasize that possibility to restrict oneself to a single dielectric-function scalar $\varepsilon_i(\mathbf{q},\omega)$ for each medium is valid only for plasma-like media (classical and quantum electron-ion plasma, dust plasma, electrolyte solutions, colloids) where any periodic crystalline structure is absent and $\varepsilon(\mathbf{q},\omega)$ does not depend on reciprocal lattice wave vectors $\vec{\mathbf{K}}$ as in solids [7]. Moreover, both for plasma-like media and solids the imaginary part of $\varepsilon''(\mathbf{q},\omega)$ exists in addition to the conventional real part $\varepsilon'(\mathbf{q},\omega)$ [1, 3 ,4]. The functions $\varepsilon''(\mathbf{q},\omega)$ describe dissipation and influence, in particular, polarization, i. e. image, forces [8] (see also next Sections). Unfortunately, even for non-magnetic, isotropic and spatially non-dispersive media adequate description of energy losses is non-trivial, since the Maxwell equations are reversible and do not make allowance for dissipation which enters via material relationships [3, 9]. For instance, the ohmic conductance is most often considered as the main source of macroscopic loss in a medium described by the Maxwell equations. On the other hand, to properly study dynamic image forces or Van der Waals

forces an account of $\varepsilon''(\mathbf{q},\omega)$ is inevitable because $\varepsilon'(\mathbf{q},\omega)$ and $\varepsilon''(\mathbf{q},\omega)$ are linked by the Kramers-Kronig relations [3, 4].

One should fully perceive that even if all media concerned are well described by their dielectric functions $\varepsilon_i(\mathbf{q},\omega)$ the very existence of a well-defined interface is a crude *approximation* which has to be justified individually for relevant specific cases. Indeed, physicists and chemists (including biophysicists and biochemists) deal with finite transitional zones between bulk media [10–13] instead of sharp interfaces of the classical electrostatics [5, 6, 14]. The electrochemical electrolyte solution-electrode boundaries are the most popular examples of such inhomogeneous structures [10, 15–17]. Therefore, in the strict sense, one should talk about the *Coulomb polarization energy* in the inhomogeneous medium rather than about the image force energy even generalized in one way or another in comparison with its classical standard form. Nevertheless, the sharp-interface approximation of interfaces is helpful in many cases at least qualitatively, so that the *image force concept* can be considered an useful and fruitful one. Moreover, the image force energy is frequently invoked as an input quantity to calculate electron energy spectra in quantum wells [18–20], tunnel currents in layered structures [21–24], photo-currents [25–28], adsorption and catalytic properties [29–33], electron microscopy [34, 35]. It should be noted that real interfaces are curved rather than flat, ion channels in biological membranes being one of the most significant examples [36–38]. Therefore, a cumbersome theory of image forces applicable to cylindrical, spherical and more exotic interfaces has been also developed [39–46].

It is worthwhile to mention that there are weak electromagnetic forces induced by quasi-neutral objects which, nevertheless, conspicuously perturb interfaces. I mean image forces induced by dipoles [29, 33, 47–52] as well as Van der Waals forces between atoms or molecules, on the one hand, and surfaces, on the other hand [53–55]. The latter interaction is used to study surface structures by means of the so-called Atomic Force Microscopy (AFM) [56–57], younger relative of the Scanning Tunnel Microscopy (STM) [58, 59] where image forces discussed here play a substantial role.

This review is not intended to cover all these flourishing activities. At the same time I would like to describe in detail what are the origin and character of image forces in practically relevant situations. Dynamic effects being important for rapidly moving charges near the interfaces [60–63] will be also discussed. The presentation includes metals (itinerant charges) and insulators (bound charges), the theory being easy to perform in the framework of the dielectric formalism [61, 64]. Of course, cumbersome mathematical expressions will be omitted in favor of physical discussion. Nevertheless, a curious reader would be able to trace all the depths of the formalism in the reference list.

Last but not least, I would like to emphasize that while studying surface phenomena one of necessity deals with small lengths of atomic or molecular order. Large organic molecules even exceed relevant lengths for which, e. g., image forces are strong enough to talk about. Therefore, in surface science physics and chemistry *can not be separated* either ideologically or practically, as is well known, in particular, in science of catalysis [65] and related issues [66, 67].

PROLEGOMENA

A point charge near a planar surface of an ideal conductor (a model of a metal in the framework of the classical electrostatics [5]) and its energy given by Eq.(1) with an accuracy of notations are shown in Fig.1 taken from Ref.[13]

This is the simplest possible electrostatic problem [5, 68]. Specifically, there is a real charge *Ze* in one medium (here it is the vacuum) and another medium, which is separated from the first one by a sharp (infinitely thin) boundary. In our case the boundary is grounded or at least equipotential. Since screening properties of various media are different, extra charges appear at the boundaries. These charges serve as additional electric field sources in the Poisson equation

$$\Delta\Phi = -4\pi\rho(\mathbf{r}) \qquad (2)$$

for the potential $\Phi(\mathbf{r})$ in the medium of interest where the initial charge is located at a point $\mathbf{r}_i$. Here $\rho(\mathbf{r})$ is the external charge density which equals $Ze\delta(\mathbf{r}-\mathbf{r}_i)$ for a point charge, whereas $\delta(\mathbf{r})$ is the Dirac delta-function. For our specific choice of coordinates $\mathbf{r}_i=(0,0,-z)$.

The problem can be solved in an indicated conventional manner for general complicated configurations of the media (bodies) involved. However, when configurations are simple enough possessing a high degree of spatial symmetry, one can introduce *fictitious* charges

situated *outside* the medium with real charges. Charges of those phantoms are selected in such a way that the resulting potentials and fields coincide with those of real boundary surface charges induced by point charges inserted into the medium concerned. Those fictitious charges are called image ones because they look like mirror images with mirror planes located at the interfaces. Image charges are always outside the region where Eq. (2) with $\rho(\mathbf{r}) = Ze\delta(\mathbf{r}-\mathbf{r}_i)$ is valid, since the particular solution of the Poisson equation must remain the same, while image or boundary charges can make contributions to the general solution of the Laplace equation which can be obtained from Eq. (2) by putting $\rho(\mathbf{r}) = 0$.

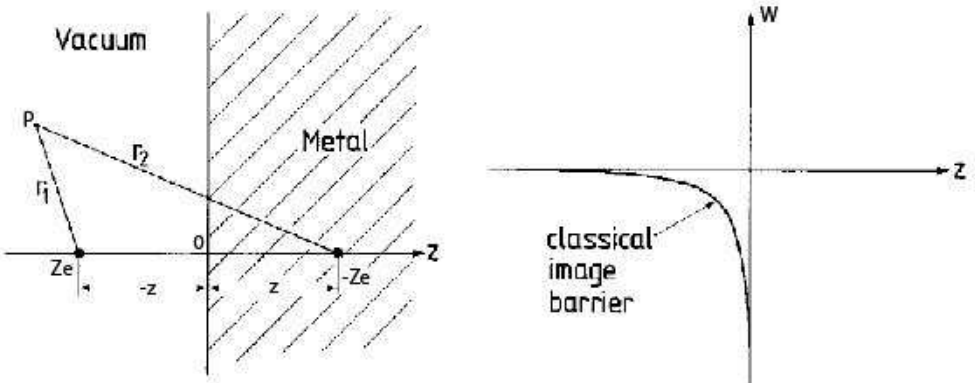

Fig. 1. (Left) A point charge outside and its image inside an ideal half-space conductor and (Right) the charge interaction energy with the polarizable interface [13].

One should bear in mind that the level of physical abstraction is *not reduced* by the substitution of point-like image charges for their distributed boundary counterparts. Indeed, continuum models of image forces fail at small distances from the conventional interfaces where their contribution becomes especially large (see Eq. (1)), since real inter-phase boundaries are neither sharp nor uniform. The atomic nature of the condensed matter is significant, in principle, and classical approach within the dielectric formalism is an approximation only. Nevertheless, the very concepts of image charges and image forces are extremely useful both for physicists and chemists, e.g. as benchmarks to check more realistic but numerical solutions. Moreover, an account of image forces gives order-of-magnitude corrections to a plenty of calculated quantities leading to much better agreement with the available experiments.

It should be noted that even if one adopts the continuum model for media and the infinitely sharp interface is considered as a satisfactory approximation, the perfect-conductor (ideal-conductor) picture has yet one more shortcoming. Namely, inherent finiteness of the screening length λ_m for electron-ion metal quantum plasma [2, 11, 15, 39, 40, 64] is also ignored. This quantity equals approximately to the inverse of the Thomas-Fermi wave number $\kappa_{TF} = (6\pi ne^2/E_F)^{1/2} \approx \cdot 10^8$ cm^{-1} where n is the electron concentration and E_F is the Fermi energy (for definiteness the relevant quantities were presented here in a free-electron approximation [6, 69]). Therefore, $\lambda_m \approx$ (0.1-0.5) nm, i.e. is comparable to the crystal lattice parameter. In the ideal-conductor model $\lambda_m = 0$. If one makes allowance for $\lambda_m \neq 0$ it means exactly the same as making allowance for the spatial dispersion of the metal dielectric function.

Given the configuration of Fig. 1 one immediately obtains the attraction force between the charge Ze and the polarizable boundary, i. e. charges induced on the metal surface,

$$F(z) = \frac{(Ze)^2}{4z^2}. \qquad (3)$$

The (negative) image force energy $W(x)$ of the charge outside the ideal conductor can be found as a work executed by the charge while moving from the infinity ($z = -\infty$) to its actual position $-z$ taken with an opposite sign

$$W(z) = -\int_{-\infty}^{-z} dzF(z) = -\frac{(Ze)^2}{4z}. \qquad (4)$$

The *r.h.s.* of Eq. (4) exactly reproduces that of Eq. (1).

One can look at Eqs. (1) and (4) from another viewpoint. Let us calculate the image force *energy* directly, bypassing antecedent calculation of the image *force*. Then

$$W(z) = -\frac{1}{2}\frac{(Ze)^2}{2z} = -\frac{(Ze)^2}{4z}. \qquad (5)$$

Here I wrote down the interaction of two charges, Ze and $(-Ze)$, separated by a distance $2z$. The *important factor* 1/2 reflects the fact that the fictitious charge $(-Ze)$ is induced itself by the test charge Ze rather than being an independent entity. Hence, the interaction energy $-(Ze)^2/2z$ of two independent charges should be divided by two in order to obtain the proper value.

There is a third way to calculate the same elementary energy $W(z)$. Specifically, let us introduce a notation $\varphi(z,Ze) \equiv Ze/2z$ for the electrostatic potential of the charge Ze at the image point. Now imagine that at first the opposite charge was equal to zero and then began to grow infinitesimally slowly until finally it took its true value $(-Ze)$. The total interaction energy between the initial charge and its image can be defined as an integral over the hypothetical charging process

$$W(z) = \int_0^{Ze} \varphi(z,\xi)\, d(-\xi) = -\int_0^{Ze} \frac{\xi}{2z}\, d\xi = -\frac{(Ze)^2}{4z}. \quad (6)$$

Here intermediate values of Ze were denoted by ξ. Of course, Eq. (6) does not differ from Eqs. (1), (4) or (5). It should be noted that my speculations in this paragraph are quite similar to those well known in electrochemistry where electrostatic components of chemical potentials for ions in electrolyte solutions were calculated using the same concept of hypothetical charging processes proposed by Güntelberg and Debye [70]. This process, in its turn, goes back to the routinely performed process of capacitor charging formally described in a like manner [5, 68, 71–73].

Since the image charge is in effect a substitute of the "more real" surface (interface, to be precise) charge $\sigma(x,y)$, it makes sense to calculate this quantity and to ascertain that the image-force picture is adequate. Analysis is easy to carry out assuming from the very beginning that the image charge $(-Ze)$ and its genuine counterpart Ze act together [71]. Let us assume that a unit vector **n**, perpendicular to the interface, is directed towards the parent charge Ze. The choice is arbitrary and a final result for $\sigma(x,y)$ does not depend on it [72]. According to the Coulomb law, a z-component E_z of the electric field, induced by the charge Ze, at a point $P = (r;\ z = 0)$ at the surface of the conductor is as follows

$$E_z^+\left(r = \sqrt{x^2+y^2}, 0\right) = \frac{Ze\cos\theta}{r^2+z^2}. \qquad (7)$$

Here r is a distance between the point P and the projection of the co-ordinate $-z$ of the charge Ze on the conductor surface whereas θ is an angle between a vector directed from Ze to P and a perpendicular to the surface. Since $\mathrm{tg}\theta = r/z$, Eq. (7) can be simplified

$$E_z^+ = \frac{(Ze)z}{\left(r^2+z^2\right)^{3/2}} \equiv E_z. \qquad (8)$$

Similarly, z-component of the image charge $(-Ze)$ equals to

$$E_z^- = -\frac{(-Ze)z}{\left(r^2+z^2\right)^{3/2}} = \frac{(Ze)z}{\left(r^2+z^2\right)^{3/2}} = E_z. \quad (9)$$

One of the consequences of the Gauss theorem is a relationship between a discontinuity of the normal component of the electric field (in our case z-components) at a charged surface and the surface charge $\sigma(x,y)$

$$E_{vac,n} - E_{conduct,n} = -E_z^+ - E_z^- = -2E_z = 4\pi\sigma(x,y). \quad (10)$$

The first equality in Eq. (10) was written down taking into account that the direction of the vector **n** coincides with that of the z-component for the image-charge electric field whereas the field of the charge Ze is in opposition to **n**. A total surface polarization charge Q is an integral over the surface of the local quantity $\sigma(x,y)$ given by Eq. (10)

$$Q = 2\pi\int_0^\infty r\,dr\,\sigma(x,y) = -Zez\int_0^\infty \frac{r\,dr}{\left(r^2+z^2\right)^{3/2}} = -Ze. \quad (11)$$

It means that our replacement of Q by the image charge was mathematically valid being, nevertheless, only a useful computational tool. By the way, it is easy to show that tangential fields of charges Ze and $-Ze$ compensate each other at any point of the surface, which is not surprising because electrical lines of force are perpendicular to conducting surfaces [5, 68, 71–73].

One should not wonder why several methods have been used to obtain such an elementary expression as Eq. (1). The answer is that the simplest possible charge configuration and the simplest possible media considered above, where image forces appear, were used as a testing ground. Now, we are ready to study much more complex situations using, however, the same basic principles and treating the textbook expression as an extremely important limiting case.

GENERALIZATIONS. STATIC IMAGE FORCES

All other kinds of image forces can be obtained as generalizations of the picture represented in the previous Section. In particular, remaining in the framework of the conventional electrostatic theory one can consider two adjacent insulators with dielectric constants ε_1 and ε_2 [5, 72, 73]. In this case free charge carriers are absent, so that $\sigma(x,y) \equiv 0$. The corresponding *non-symmetrical* electrostatic problem is solved taking into account continuity of normal displacement components and tangential field components. The resulting expression for the image force energy has the form

$$W_1(z) = -\frac{(Ze)^2(\varepsilon_2 - \varepsilon_1)}{4z\varepsilon_1(\varepsilon_2 + \varepsilon_1)}. \qquad (12)$$

Here, for the sake of definiteness, the energy was written down for medium 1 while for medium 2 the energy is given by the same formula with an accuracy of interchanged subscripts 1 and 2. For a charge in the vacuum near a metal half-space Eq. (1) can be reproduced by ε_2 tending to infinity and $\varepsilon_1 = 1$. Indeed, in the phenomenological electrostatics ideal conductors correspond to $\varepsilon \to \infty$. The expression (12) demonstrates that a charge should approach a medium with larger dielectric constant to lower its energy.

Image force energies (1) and (12) in the vacuum or in an insulator near another medium can be generalized in a straightforward way to the case of a slab between covers with differing dielectric functions. Of course, the latter may possess spatial (**k**) and temporal (ω) dispersion (see Fig. 2 where either possible non-relativistic motion of the charge or its rest is considered on an equal footing).

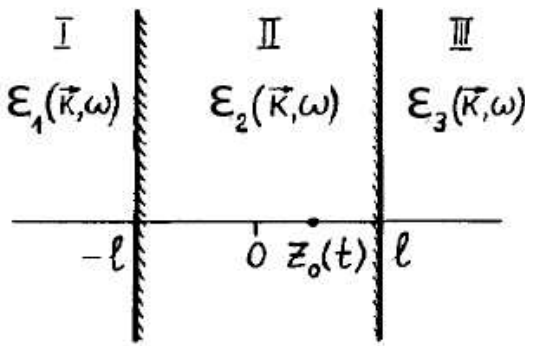

Fig. 2. Charge moving, according to the equation $z = z_0(t)$, or quiescent in a three-layer system [61].

It is evident that the image force energy inside the sandwich is *not a superposition* of contributions from image charges induced in both covers. Indeed, each image charge form one cover is "reflected" in another cover while this reflection, in its turn, induces a charge in the first cover. Therefore, one has an infinite series which can be summed analytically in the simplest cases [5, 61]. Otherwise the resulting image force energy is calculated numerically. On the other hand, it is not necessary to directly use the image method in a slab where its simplicity is lost. It is more convenient to solve the electrostatic (quasi-electrostatic, for slowly moving charges) problem [48, 61] with continuity boundary conditions mentioned above [5, 72, 73]. Needless to say, the results coincide for both methods. Moreover, similar expressions in the static case can be obtained in a less transparent but more general technique of the Coulomb Green's functions [64].

Image forces in the configuration displayed in Fig. 2 are significant to study electrical and optical phenomena in hetero-structures [18, 19], metal-oxide-semiconductor [23] and metal-oxide-metal [22] devices in electronics, electrolytic liquid crystal cells [31, 74] or double-walled nanotubes [45]. Sometimes even adsorbate layers are described as dielectric slabs in the constant approximation for their dielectric functions [66].

It is worthwhile to demonstrate some expressions for the image force energy in the interlayer $W_2(z)$ in the approximation of the classical electrostatics. Let us restrict ourselves to the symmetric sandwich with $\varepsilon_1 = \varepsilon_3 = \varepsilon = \text{const}$ and $\varepsilon_2 = \text{const} \neq \varepsilon$ [61]

$$W_2(z) = -\frac{(Ze)^2 \ln(1+\eta)}{2l\varepsilon_2} + U(z); \qquad (13)$$

$$U(z) = -\frac{\eta(Ze)^2}{4\varepsilon_2 l}\int_0^1 \frac{ds}{1-\eta^2 s^2}\left(s^{z/l} + s^{-z/l} - 2\right); \qquad (14)$$

$$\eta = \frac{(\varepsilon - \varepsilon_2)}{(\varepsilon + \varepsilon_2)}. \qquad (15)$$

As can be seen from Eqs. (13)–(15), the interplay between images has nothing to do with simple summation of two single-boundary image force energies. It is especially well seen if one makes an approximation of the integral (14) valid with an accuracy of 6% so that [61]

$$U(z)=-\frac{\eta(Ze)^2 z^2}{2\varepsilon_2 l\left(l^2-z^2\right)}=-\frac{\eta(Ze)^2 z}{4\varepsilon_2 l}\left(\frac{1}{l-z}-\frac{1}{l+z}\right). \quad (16)$$

A term with the logarithm in Eq. (13) can be properly called an interference one embodying the contributions of different images of all orders.

The exact result (13)–(15) tends to the expression of the classical electrostatics [5] for $\varepsilon \to \infty$ and $\varepsilon_2 = 1$

$$W_{class-cond}(z)=\frac{(Ze)^2}{8l}\left[2\ln\gamma+\psi\left(\frac{1}{2}-\frac{z}{2l}\right)+\psi\left(\frac{1}{2}+\frac{z}{2l}\right)\right] \quad (17)$$

where γ =1.78… is the Euler constant and $\psi(x)$ is the di-gamma function. One should note that a well-known and widely used Simmons's analytical approximation [75] of (17) is not correct and should be replaced by our Eqs. (13), (16) with $\varepsilon \to \infty$ and $\varepsilon_2 = 1$.

The main shortcoming of all expressions for $W(x)$ presented above is their divergence near the interfaces. It is not crucial for the macroscopic electrostatics where relevant distances from metallic or semiconducting electrodes exceed all characteristic lengths of the problem. On the other hand, typical problems of emission electronics, catalysis, and biophysics of ion channels in cell membranes require more or less exact expressions for image forces at 0.5–10 nm distances. Hence, various physical reasons leading to finiteness of $W(x)$ were found and the corresponding physical models were elaborated. I would like to mention only the most significant ones.

The first step to avoid singularities is to shift the denominator in Eq. (1)

$$W_{shift}(z) = -\frac{(Ze)^2}{4\left(z+\bar{z}\right)}. \quad (18)$$

Here $\bar{z}$ is a phenomenological length (remember that both z and $\bar{z}$ are positive!) introduced in such a way that $W_{shift}(0)$ is finite at the interface. Of course, there was at first no microscopic justification of Eq. (18) although the results turned out to be rather satisfactory [76].

Another consideration ensuring a saturation of the image force energy at the interfaces is based on the trivial but important in this context fact that the Coulomb field in a metallic sample is totally screened at a final distance λ_m from the surface, contrary to what is assumed in the electrostatics of ideal conductors. I have already indicated that the simplest model, which describes this circumstance, is a Thomas-Fermi one [15, 64, 66]. For this model, the static dielectric permittivity $\varepsilon(\mathbf{q},0)$ takes the form

$$\varepsilon_{TF}(\mathbf{q},0)=1+\frac{\kappa_{TF}^2}{q^2} \quad (19)$$

where κ_{TF} is the Thomas-Fermi wave number introduced in the previous section. Then, using the same routine methods of solving the Poisson equations with the indicated above continuity relations, one can obtain the whole profile of $W_{TF}(z)$ both in vacuum and metal [64, 77]. The vacuum branch of $W_{TF}(z)$ is the generalized image force energy with the sought-for saturation at the metal-vacuum interface: $W_{TF}(0) = -(Ze)^2\kappa_{TF}/3$. At the same time, $W_{TF}(z)$ inside the metal is no longer the infinite well of the classical electrostatics characterized by the dielectric constant $\varepsilon \to \infty$. On the contrary, it is a finite internal potential energy $W_{TF}(z \to \infty) = -(Ze)^2\kappa_{TF}/2$, in other words, a bottom of the conduction band (such an interpretation becomes valid if we abandon generality and put $Z = 1$). This quantity is reckoned from the zero-value vacuum energy level and is of the order of several electron-volts in magnitude both in the primitive semi-classical Thomas-Fermi approximation and in any of sophisticated quantum-mechanical approaches. A transition between $W_{TF}(0)$ and $W_{TF}(z \to \infty)$ takes place in a tiny interval $\sim \kappa_{TF}^{-1}$.

Those concepts may be applied to more realistic models of a metal and its surface. In this case, the internal potential energy and the very dependence $W(z)$ in the entire range $-\infty < z < \infty$, whatever model of metal is used, include both the electrostatic part $e\varphi_{el}(z)$ and the exchange-correlation term $\mu_{xc}(z)$ contributing to the one-electron chemical potential μ of the electron liquid (once more, pay attention that here the generality adopted earlier is absent and $Z = 1$!). One of the drawbacks of the Thomas-Fermi theory is a neglect of many-body term $\mu_{xc}(z)$, so that $W(z)$ and $e\varphi_{el}(z)$ coincide and the work function equals to zero [78].

Unfortunately, Thomas-Fermi-approximation formula (19) for the electron-gas dielectric function which substantially improves the description of the surface properties, is insufficiently satisfactory, since a derivative of $W_{TF}(z)$, i. e. the image force itself $F_{TF}(z)$ logarithmically diverges at the interface [64, 77]

$$\frac{\partial W_{TF}(z)}{\partial z} \to \ln\left(\kappa_{TF}|z|\right) \text{ for } |z| \to 0\,. \quad (20)$$

The reason is that the quasi-classical (Thomas-Fermi) theory of matter does not take into account (i) electron-electron correlations and (ii) quantum-mechanical interference of the electron wave functions [79, 80]. At the same time, the Thomas-Fermi theory is based on the Pauli principle and the Fermi-Dirac statistics that are enough to describe metal properties for small wave vectors **q** (large lengths, in the spirit of the Fourier-transformation ideology).

However, for large wave vectors $q \approx k_F \approx 10^8$ cm^{-1} the corresponding distances $\sim q^{-1}$ become comparable with crystal lattice constants and the electron de Broglie wavelength $2\pi\hbar/mv_F$. Here $v_F \approx 10^8$ cm/s is the electron velocity at the Fermi surface, $k_F = (3\pi^2 n)^{1/3}$ is the Fermi wave vector, and m is the electron mass (here, for definiteness, I am reasoning in terms of the free-electron model). Then the quantum-mechanical effects become significant. Nevertheless, in many cases calculated and measured quantities are integrals over q, so that one can restrict the consideration to the quasi-classics. Such arguments fail for interfacial phenomena where we are interested in the system behavior for *small distances* from the boundaries, i. e. for large q!

A proper expression for the dielectric function of a metal making allowance for quantum effects was obtained by Lindhard in his famous article [80]. In the static limit when $\omega/kv_F \to 0$, the Lindhard dielectric static permittivity takes the form

$$\varepsilon_L(\mathbf{q}) = 1 + \frac{4\pi e^2}{q^2}\Pi(\mathbf{q}) \quad (21)$$

where $\Pi(\mathbf{q})$ is the polarization operator

$$\Pi(\mathbf{q}) = N(k_F)\left[1 + \frac{1-s^2}{2s}\ln\left|\frac{s+1}{s-1}\right|\right]. \quad (22)$$

In Eq. (22) $N(k_F) = mk_F/2\pi^2\hbar^2$ is the electron density of states per spin direction at the Fermi level, whereas $s = q/2k_F$. Eq. (22) is valid (in the free-electron approximation!) for arbitrary wave vectors (momenta).

The quantum-mechanical permittivity (21)–(22) has two peculiarities as compared to the quasi-classical one (19). The first one is a logarithmic peculiarity of the polarization operator at $q = 2k_F$. Being *prima facie* weak it, nevertheless, leads to a substantial modification of the itinerant electron screening cloud at large distances. Namely, the so-called Friedel oscillations of the form $\cos(2k_F r)/r^m$ appear at $r >> k_F^{-1}$ as well as concomitant (Kohn) anomalies of the metal phonon spectra at $q \approx 2k_F$ [69]. Here a power exponent m depends on the shape of the Fermi surface [64]. The Friedel oscillations, in particular, manifest themselves in the electron density of metals near the surface, so that the validity of the corresponding smooth Thomas-Fermi-like behavior is out of the question.

The other quantum-mechanical effect is the large-q fast reduction of $[\varepsilon(\mathbf{q}) - 1]$:

$$\varepsilon_L(\mathbf{q}) \approx 1 + \frac{4\kappa_{TF}^2 k_F^2}{3q^4} \text{ at } q >> k_F\,. \quad (23)$$

Because of the property (23) the usage of Eq. (21)–(22) instead of Eq. (19) results in a continuity of both $W_{TF}(z)$ and $\partial W_{TF}(z)/\partial z$ at the interface, so that the solid state theory allows to eliminate the unphysical singularity of the classical electrostatics.

The same is true for the boundaries between different kinds of insulators and semiconductors which is extremely important, e.g., for biological tissues. The latter from the point of view of their electrical conductivity can be considered as a network of insulating membranes and channels filled by electrolyte solutions [36]. The classical formula (12) should be modified there in a similar way as it happens for its "metallic" counterpart (1). The revolutionary idea belongs to Inkson [81] who understood that the dielectric function for an insulator $\varepsilon(\mathbf{q})$ becomes the static dielectric constant ε_0 (over the optical frequency range, as is well known [1, 9, 15, 19, 69], a proper screening constant is $\varepsilon_\infty < \varepsilon_0$) only for large distances from a test charge or other electric field source, i. e. for small enough q. On the other hand, at small distances (large q) $\varepsilon(\mathbf{q})$ should tend to unity similarly to what is appropriate for metals (see Eqs. (19), (23)). Therefore, an interpolation expression was suggested

$$\varepsilon_I(\mathbf{q}) = 1 + \frac{\varepsilon_0 - 1}{1 + \frac{q^2}{\kappa_S^2}(\varepsilon_0 - 1)} \quad (24)$$

where κ_S is the effective screening length by valence electrons described in that sense as itinerant ones. I emphasize that this equation is consistent with the classical electrostatics in the range of its validity, i.e. at $q \to 0$. At the same time, at large q

(small distances) all bound charges become effectively free which justifies Thomas-Fermi-like treatment of the valence electrons.

Eq. (24) has as bad asymptotic at large q as its analogue (19). In particular, this drawback leads to a finite $W_I(z \to 0)$ while $\partial W_I(z)/\partial z$ diverges near the interface. Schulze and Unger improved the input bulk semiconductor properties and constructed [82] a phenomenological $\varepsilon_{SU}(\mathbf{q})$ which has the same asymptotic (23) as $\varepsilon_L(\mathbf{q})$

$$\varepsilon_{SU}(\mathbf{q}) = 1 + \frac{\varepsilon_0 - 1}{1 + \frac{q^2}{\kappa_S^2}(\varepsilon_0 - 1)} \times \frac{1}{1 + \frac{3q^2}{4k_S^2}}. \quad (25)$$

Here k_S is the Fermi momentum of the semiconductor valence electrons considered as free ones. We showed [62, 83] that a choice of $\varepsilon_{SU}(\mathbf{q})$ as dielectric function while calculating image force energies $W_{SU}(z)$ removes the divergences, thus qualitatively solving the problem concerned. The results shown in Fig. 3 are taken form Ref. [62]. Pay attention that here vacuum half-space is located at positive z.

One readily sees that the discrepancies between the models are large in the neighborhood of a semiconductor-vacuum interface and the use of the Schulze-Unger model is preferable. Similar conclusions can be made in the case of vacuum interlayers between semiconducting electrodes [62].

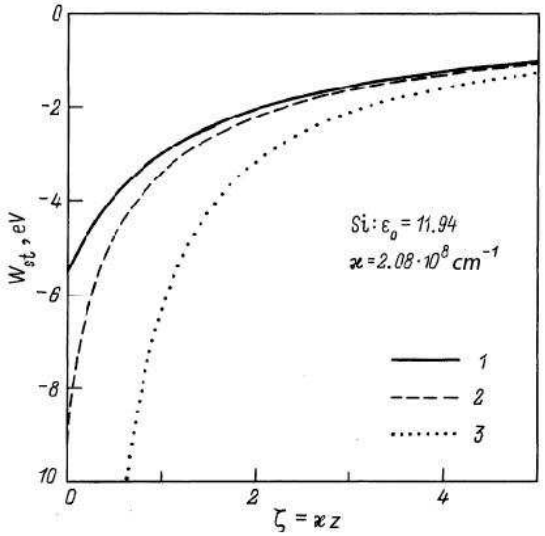

Fig. 3. Profiles of image force energies for different models of semiconducting silicon. 1 – Schulze-Unger model, 2 – Inkson model, 3 – classical electrostatic model [62].

In the cases of doped semiconductors or electrolyte solutions there are two main contributions to the overall dielectric function [74, 84]. The Debye-Hückel term is the first one having the same form as the Thomas-Fermi inverse screening length (19). However, the Debye-Hückel screening constant is a temperature-, T, dependent one. For 1:1 electrolyte, e. g., the latter is $\kappa_{DH} = (8\pi N e^2/k_B T\varepsilon_e)^{1/2}$ where N is a concentration of each ion component, k_B is the Boltzmann constant, ε_e is the solvent macroscopic static dielectric constant. A q-dependent polarization function of the solvent being of the same nature as the semiconductor Inkson function, constitutes the second contribution.

Interplay between dielectric functions of neighboring electrode and electrolyte solution may lead to extra ion adsorption Γ of either sign depending on the system parameters [84] (Fig. 4).

If one intentionally deposits an interlayer its dielectric function and thickness may change Γ sign. In the case of liquid crystal displays this role often plays a polymer film which via changing of image forces prevents ion adsorption (sticking effect), thus improving display characteristics [74]. The electrostatic excess ad-sorption Γ crucially depends on the relationship between the liquid (liquid crystalline) solvent ε_e and that of the interlayer.

In the case of a metal-vacuum boundary another, more powerful, self-consistent method was used to calculate the entire spatial behavior of the potential charge energy across the interface from the metal bulk (internal potential) to the vacuum (image force energy) [78, 85, 86]. Similar technique was also applied to the electrochemical interface between a metal electrode and an electrolyte solution [11, 15]. All models used in those cases can be roughly divided into two groups: (i) jellium-like ones where ions are treated as compensating positive structureless background; and (ii) models explicitly making allowance for a periodic crystal lattice. Analysis carried out in the framework of different approaches supports our understanding obtained on the basis of more simple treatments. Self-consistent quantum-mechanical approaches are, however, much more successful in quantitative calculations [86, 87].

Another feature deserves to be mentioned – due to the $2k_F$ peculiarity of the Lindhard function (21), (22) (also appropriate to more sophisticated dielectric functions, taking into account electron-electron correlations [88]), self-consistently calculated electron density $n(z)$ and (to a lesser extent) the potential energy $W(z)$ exhibit the Friedel

oscillations inside the metal. This feature preserves if one explicitly takes into account the discrete nature of the ionic background. Of course, in the latter case the electron potential energy $W(z)$ reflects the periodicity of the ion-core potential profile in the bulk, reaching, on the other hand, the smooth image-force energy in the vacuum. The behavior of $W(z)$ in the surface region determines the observed surface characteristics of metals and electrolyte cells, including work functions [11, 15, 86, 87]. As an example, dependences of $W(z)$ and its electrostatic constituent $e\varphi_{el}(z)$ are shown in Fig.5. One sees that the realistic image-force behavior is rather smooth without any surface singularity inherent to naïve considerations, although the classical behavior (1) is rapidly restored in the vacuum region.

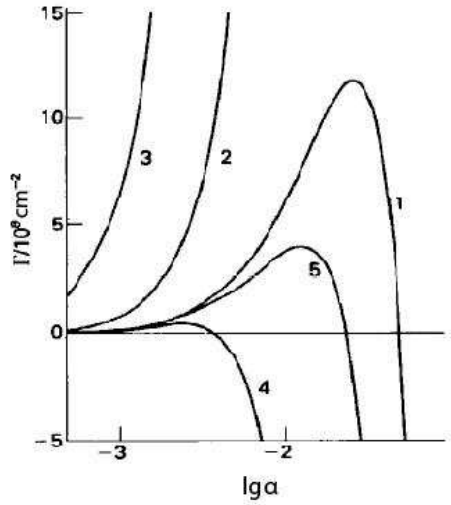

Fig. 4. Dependence of the excess image-forces-induced surface adsorption Γ on dimensionless parameter $\alpha \equiv e^2\kappa_{DH}/2k_BT\varepsilon_e \sim \sqrt{N}$ for the Hg/aqueous electrolyte solution interface. Curves l-3 correspond to the Taylor model for the metal taking into account electron-electron correlations and κ_S = 0.3 nm, 0.5 nm and 1 nm, curve 4 corresponds to the Thomas-Fermi approximation for metal and κ_S = 0 (Debye-Hückel model) and curve 5 corresponds to the Thomas-Fermi approximation and κ_S = 0.3 nm [84].

An interesting generalization arises if one considers a micro-charge Ze which polarizes a dielectric sphere without [43] or with [39] spatial dispersion of its permittivity rather than a plane interface. The problem is difficult even from the technical viewpoint because the polarization in the spherical interface case cannot be formulated as an interaction with a fictitious image charge, i. e. a number of image charges becomes infinite as, e. g., in the case of a charge in vacuum between two metallic half-spaces [5]. One of the main conclusions is that the strength of image forces in spherical geometry is considerably smaller than at vanishing curvature [46]. The model was advantageously applied to colloidal particles and polyelectrolytes [46].

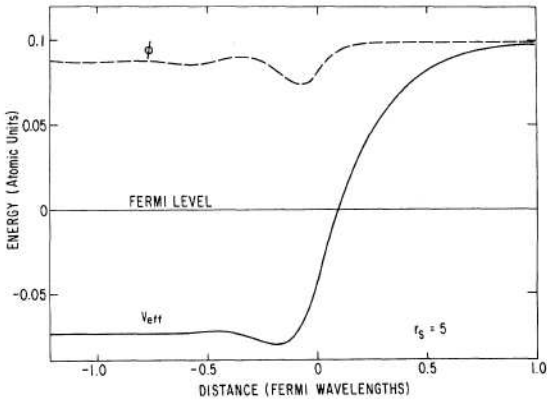

Fig. 5. Spatial dependences of the electron energy $W(z)$ and its electrostatic constituent $e\varphi_{el}(z)$ near a metal-vacuum interface (vacuum is to the right). Ion lattice is approximated by a positive background [89].

DYNAMICAL EFFECTS. SURFACE PLASMONS AS A SOURCE OF IMAGE FORCES

The self-consistent theory [78, 85, 89] which directly involves renormalization of the one-electron quasiparticle spectrum by many-body effects due to the electron interaction with its environment (condensed phases), should involve contributions to physical quantities not only from one-particle Fermi excitations of relevant media but from their collective Bose excitations as well [90]. In order to isolate the collective excitations that in our case with its explicit electrostatic interaction must be plasmons, i. e. electromagnetic oscillations in the bulk and at the interfaces between media involved one should deal with the non-local self-energy $\Sigma(\mathbf{r}, \mathbf{r}', \omega)$ (responsible for electron exchange and correlation). Such a program was realized in the framework of the model with sharp interfaces and bulk dielectric functions [91]. In particular, for a hydrodynamic $\varepsilon(\mathbf{q},\omega)$

$$\varepsilon_{MH}(\mathbf{q},\omega) = 1 + \frac{\kappa_{TF}^2}{q^2 - \left(\omega/\omega_p\right)^2 \kappa_{TF}^2} \qquad (26)$$

being a long-wavelength approximation of the Lindhard dynamic permittivity [80, 90], relevant bulk excitations are bulk plasmons whereas at the metal-vacuum interfaces the surface plasmons with frequency $\omega_s = \omega_p/\sqrt{2}$ are decisive factors. Here, in the free-electron approximation the Langmuir plasma frequency is $\omega_p = \sqrt{4\pi ne^2/m}$ and m is the electron mass.

The screened interaction energy, taking into account $\Sigma(\mathbf{r}, \mathbf{r}', \omega)$ and based on Eq. (26), tends to the image potential energy in the vacuum region far away from the metal surface which confirms, at least, qualitative validity of the calculation. Moreover, this approach can be easily applied to other solid media, e. g. semiconductors [92]. Since the polarization energy (image force energy) thus obtained is *static* and the surface plasmons are its source, the static image forces origin might be interpreted as an interaction of an electron (or other test charge) with zero-point oscillations of virtual surface plasmons [93, 94]. From this viewpoint, the surface charge $\sigma(x,y)$ of the classical electrostatics involved into Eqs. (10), (11) can be considered as a frozen surface plasmon. Of course, this identification is not exact. Indeed, the dependence $W(z)$ is integral including contributions *both from surface and bulk* plasmons. The latter is of a minor importance for the outer region of $W(z)$, i. e. for the image force energy *per se*, while the inner (intra-metal) branch of $W(z)$ is formed by the surface and bulk terms together with the internal potential energy determined by the bulk plasmons alone [94].

Now we can generalize our treatment and assume a finite velocity v of the charge Ze, located at a moment t at a point $z_0(t)$ (see Fig. 3, where a three-layer configuration is depicted). The trajectory is supposed to be perpendicular to the interfaces. Such an approach was suggested previously [48, 95–97], the electron motion being non-relativistic, i. e. $v \ll c$, where c is the light velocity. It means that one can totally neglect *the retardation of the electromagnetic potentials* whereas *the inertia of the plasma response* becomes essential. Indeed, in the latter case small parameters which characterize the importance of the dynamic corrections to the static image forces in a close vicinity of the interfaces $z \to 0$, are as follows [61]

$$\kappa_{TF}^2 v^2/\omega_p^2 \qquad (27)$$

if a charge moves with a constant speed v and

$$e\kappa_{TF}E_{ext}/m\omega_p^2 \qquad (28)$$

if a charge is accelerated in the external field E_{ext}. At a large distance z from the interface in the vacuum region, the small parameters remain the same with an accuracy of a substitution $\kappa_{TF} \to z^{-1}$. The emergence of the dynamical perturbation of the image forces is due to finiteness of the plasma frequency ω_p. Namely, itinerant electrons inside a metal simply have no time to properly screen a varying field of a moving charge. Eqs. (27), (28) confirm the statement made above that the plasmon retardation has little to do with the electromagnetic relativistic retardation. In fact, these formulae do not contain the light velocity c whereas the plasma frequency ω_p appears there.

It can be shown that in fields, smaller than atomic ones $m^2e^5/\hbar^4$, the correction (28) for a typical metal is of the order 0.05 [61]. On the other hand, if a velocity v becomes of the order of a metal Fermi velocity $v_F \sim 10^6$ m/s, parameter (27) is no longer small. However, in this case one can forget about the spatial dispersion of $\varepsilon(\mathbf{q},\omega)$ altogether and still arrive at the exact solution for image force energies with *the finite value* at $z = 0$ [48, 95, 97]! It means that the singularity can be eliminated by the temporal dispersion alone, so that for incident charged particles, i. e. traveling *from vacuum* perpendicularly to a metal surface one obtains:

$$W\left[z_0(t)\right] = -\frac{(Ze)^2}{2v} f\left(\frac{2\omega_s \left|z_0(t)\right|}{v}\right) \qquad (29)$$

where

$$f(x) = \mathrm{Ci}(x)\sin x - \mathrm{si}(x)\cos x, \qquad (30)$$

$$\mathrm{Ci}(x) = -\int_x^\infty \frac{\cos t}{t} dt, \qquad (31)$$

$$\mathrm{si}(x) = -\int_x^\infty \frac{\sin t}{t} dt. \qquad (32)$$

At the interface from Eqs. (29) and (30) it comes about that the announced finite value becomes

$$W(0) = -\frac{\pi(Ze)^2\omega_s}{4v} \qquad (33)$$

while at the large distances from the metal surface $2\omega_s \left|z_0(t)\right|/v >> 1$ the classical (quasi-static) image force energy (1) is restored with $z = z_0(t)$.

Quite another situation emerges, when charged particles are *emitted* from a metal into the vacuum with a constant velocity v normal to the interface, as in the previous example. Specifically, in this case the emission is accompanied by the excitation of *real* surface plasmons leading to the different behavior of $W(z)$. Namely, even at far distances from the metal classical image forces are distorted by oscillating terms of the same order of magnitude [48]. This unphysical behavior is, however, an artifact caused by the neglect of the plasmon damping always existing although not always substantial. The metal dielectric function in this case (without spatial dispersion!) takes the form

$$\varepsilon_{plasm}(\mathbf{q},\omega) = 1 - \frac{\omega_p^2}{\omega(\omega + i\rho)} \qquad (34)$$

where ρ is the inverse relaxation time characterizing the damping of the plasma oscillations. For incident particles the damping is not crucial indeed, whereas for emitted charges it leads to the suppression of anomalous terms and the restoration of the good old image force energy [8]

$$W_{emit}(|z_0(t)| \to \infty) = -\frac{(Ze)^2}{4|z_0(t)|}\left\{1 - \exp\left(-\frac{\rho|z_0(t)|}{2v}\right)\times\right.$$

$$\left.\left[2\cos\frac{\Omega_s|z_0(t)|}{v} + \frac{\rho}{\Omega_s}\left(1 - \frac{2v}{\rho|z_0(t)|}\right)\sin\frac{\Omega_s|z_0(t)|}{v}\right]\right\}. \qquad (35)$$

Here

$$\Omega_s = \sqrt{\frac{\omega_p^2}{2} - \frac{\rho^2}{4}} \qquad (36)$$

is the renormalized surface plasma frequency. Nevertheless, a strong influence of the real plasmons on the $W(z)$ behavior at the intermediate distances from the interface survives the damping effect.

Dynamical renormalization of the image forces is not a kind of exotics. On the contrary, field emission processes, where electrons are emitted and accelerated in vacuum, inevitably involve the *dynamic* image forces [61, 62, 98]. Incomplete screening of the emitted-charge field by the retarded plasma oscillations leads to broadening of the corresponding tunnel barrier, so that the current becomes smaller than that given by the conventional Fowler-Nordheim theory [6, 32]. Such a reduction was observed, e. g., in photon-assisted tunneling [99].

CONCLUSIONS

The facts and speculations covered by this paper show that the image force concept which appeared as a technical tool used to tackle cumbersome electrostatic problems, has transformed into a flourishing research realm. Based on the concept concerned, self-consistent approach (using the electron density functional), dielectric formalism, quantum-field-theory methods describing the interaction between charges and surface plasmons were applied to study solid-state electronics, atmospheric science, electrochemical surface, biological membranes, catalytic reactions, scanning tunnel microscopy, atomic force microscopy. I would like to mention, in particular, such exotic spheres of applicability of the image force concept as oxide growth and the crystal defect behavior [100] and deposition of multiply charged particles on wire screens [101]. Although modern theoretical methods are quite sophisticated, it is now easier for experimentalists to interpret their results on the basis of the image-force concept than it was decades ago. Better understanding of the microscopic background of the classical notion is the reason of this success in the research. Here, I tried to elucidate only main ideas leaving the technical side of the problem beyond the scope of the paper. The reader can find necessary details in numerous references, reflecting various, sometimes conflicting viewpoints.

I am grateful to the 2008 and 2009 Visitors Programs of the Max Planck Institute for the Physics of Complex Systems (Dresden, Germany) for giving me opportunity to work on the subject in a quiet and stimulating atmosphere. Remarks and suggestions of the anonymous Referee of the Journal are also acknowledged with gratitude.

REFERENCES

1. *Agranovich V.M., Ginzburg V.L.* Crystal Optics with Spatial Dispersion and Exciton Theory. – N.-Y.: Springer, 1984. – 455 p.
2. *Halevi P.* Spatial Dispersion in Solids and Plasmas / Ed. P. Halevi. – Amsterdam: Elsevier, 1992. – 681 p.
3. *Ginzburg V.L.* Theoretical Physics and Astrophysics. – M.: Nauka, 1987. – 488 p. (in Russian).

4. *Pamyatnykh E.A., Turov E.A.* Foundations of the Material Medium Electrodynamics in Alternating and Nonhomogeneous Fields. – M.: Fizmatlit, 2000. – 240 p. (in Russian).
5. *Smythe W.R.* Static and Dynamic Electricity. – N.-Y.: McGraw-Hill, 1950. – 648 p.
6. *Dobretsov L.N., Gomoyunova M.V.* Emission Electronics. – M.: Nauka, 1966. – 564 p. (in Russian).
7. *Bechstedt F.* Electronic relaxation effects in core level spectra of solids // Phys. Status Solidi B. – 1982. – V. 112, N 1. – P. 9–49.
8. *Gabovich A.M., Rozenbaum V.M., Voitenko A.I.* Importance of the plasmon damping for the dynamical image forces // Phys. Status Solidi B. – 1999. – V. 214, N 1. – P. 29–33.
9. *Lyubimov Yu.* A. Studies on History of Electromagnetism and Dielectrics. – M.: Binom. Laboratory of Knowledge, 2008. – 376 p. (in Russian).
10. *Rice S.A., Guidotti D., Lemberg H.L. et al.* Some comments on the electronic properties of liquid metal surfaces // Adv. Chem. Phys. – 1974. – V. 27. – P. 543–633.
11. *Feldman V.J., Partenskii M.B., Vorob'ev M.M.* Surface electron screening theory and its applications to metal-electrolyte interfaces // Prog. Surf. Sci. – 1986. – V. 23, N 1. – P. 3–154.
12. *Nakamura T.* Modification of the image potential for the interfacial zone with varying dielectric constant // J. Phys. Soc. Jpn. – 1983. – V. 52, N 3. – P. 973–980.
13. *Jennings P.J., Jones R.O.* Beyond the method of images – the interaction of charged particles with real surfaces // Adv. Phys. – 1988. – V. 37, N 3. – P. 341–358.
14. *Feibelman P.J.* Surface electromagnetic fields // Prog. Surf. Sci. – 1982. – V. 12, N 4. – P. 287–408.
15. *Vorotyntsev M.A., Kornyshev A.A.* Electrostatics of Media with Spatial Dispersion. – M.: Nauka, 1993. – 240 p. (in Russian).
16. *Boguslavsky L.I.* Bioelectrochemical Phenomena and the Interface. – M.: Nauka, 1978. – 360 p. (in Russian).
17. *Halley J.W., Walbran S., Price D.L.* Chemical physics of the electrode-electrolyte interface // Adv. Chem. Phys. – 2001. – V. 116. – P. 337–387.
18. Coon D.D., Liu H.C. Image force effects in heterostructures and quantum-wells // Superlattices Microstruct. – 1987. – V. 3, N 1. – P. 95–98.
19. *Pokatilov E.P., Fomin V.M., Beril S.I.* Oscillatory Excitations, Polarons and Excitons in Multilayer Systems and Superlattices. – Kishinev: Shtiintsa, 1990. – 280 p. (in Russian).
20. *Gámiz F., Cartujo-Cassinello P., Jiménez-Molinos F. et al.* Influence of image force and many-body correction on electron mobility in ultrathin double gate silicon on insulator inversion layers // Appl. Phys. Lett. – 2003. – V. 83, N 15. – P. 3120–3122.
21. *Ossicini S., Bertoni C.M.* Image-force effects on the barrier height for metal-metal tunneling electrons // Phys. Rev. B. – 1987. – V. 35, N 2. – P. 848–850.
22. *Ma X.C., Shu Q.Q., Meng S., Ma W.G.* Image force effects on trapezoidal barrier parameters in metal-insulator-metal tunnel junctions // Thin Solid Films. – 2003. – V. 436, N 2. – P. 292–297.
23. *Quan W.Y., Kim D.M., Cho M.K.* Unified compact theory of tunneling gate current in metal-oxide-semiconductor structures: Quantum and image force barrier lowering // J. Appl. Phys. – 2002. – V. 92, N 7. – P. 3724–3729.
24. *Akkerman H.B., Naber R.C.G., Jongbloed B. et al.* Electron tunneling through alkanedithiol self-assembled monolayers in large-area molecular junctions // PNAS. – 2007. – V. 104, N 27. – P. 11161–11166.
25. *Arafune R., Hayashi K., Ueda S., Ushioda S.* Energy loss of photoelectrons by interaction with image charge // Phys. Rev. Lett. – 2004. – V. 92, N 24. – P. 247601–247605.
26. *Jensen K.L.* Time dependent models of field-assisted photoemission // J. Vac. Sci. Technol. B. – 2005. – V. 23, N 2. – P. 621–631.
27. *Godlewski J.* Currents and photocurrents in organic materials determined by the interface phenomena // Adv. Colloid Interface Sci. – 2005. – V. 116, N 1–3. – P. 227–243.
28. *Afanas'ev V.V., Stesmans A.* Internal photoemission at interfaces of high-κ insulators with semiconductors and metals // J. Appl. Phys. – 2007. – V. 102, N 8. – 081301/1–28.
29. *Badiali J.P., Forstmann F.* Long-range correlation between polar molecules adsorbed onto a dielectric solid // Chem. Phys. – 1990. – V. 41, N 1. – P. 63–78.
30. *Nakatsuji H., Nakai H., Fukunishi Y.* Dipped adcluster model for chemisorptions and catalytic reactions on a metal-surface - image

force correction and applications to Pd-O_2 adclusters // J. Chem. Phys. – 1991. – V. 95, N 1. – P. 640–647.
31. *Barbero G., Evangelista L.R.* Adsorption Phenomena and Anchoring Energy in Nematic Liquid Crystals. – Boca Reton (Florida): Taylor and Francis, 2006. – 352 p.
32. *Modinos A.* Field, Thermionic and Secondary Electron Emission Spectroscopy. – N.-Y.: Plenum Press, 1984. – 375 p.
33. *Huang H., Manciu M., Ruckenstein E.* The effect of surface dipoles and of the field generated by a polarization gradient on the repulsive force // J. Colloid Interface Sci. – 2003. – V. 263, N 1. – P. 156–161.
34. *Echenique P.M., Howie A.* Image force effects in electron-microscopy // Ultramicroscopy. – 1985. – V. 16, N 2. – P. 269–272.
35. *Rivacoba A., Zabala N., Aizpurua J.* Image potential in scanning transmission electron microscopy // Prog. Surf. Sci. – 2000. – V. 65, N 1-2. – P. 1–64.
36. *Kuyucak S., Sparre Andersen O., Chung S-H.* Models of permeation in ion channels // Rep. Prog. Phys. – 2001. – V. 64, N 11. – P. 1427–1472.
37. *Zhang J., Kamenev A., Shklovskii B.I.* Conductance of ion channels and nanopores with charged walls: A toy model // Phys. Rev. Lett. – 2005. – V. 95, N 14. – 148101/1–4.
38. *Kamenev A., Zhang J., Larkin A.I., Shklovskii B.I.* Transport in one-dimensional Coulomb gases: From ion channels to nanopores // Physica. A. – 2006. – V. 359. – P. 129–161.
39. *Vorotyntsev M.A.* Model nonlocal electrostatics: II. Spherical interface // J. Phys. C: Solid State. – 1978. – V. 11, N 15. – P. 3323–3331.
40. *Kornyshev A.A., Vorotyntsev M.A.* Model nonlocal electrostatics: III. Cylindrical interface // J. Phys. C: Solid State. – 1979. – V. 12, N 22. – P. 4939–4946.
41. *Ohshima H.* Electrostatic interaction between a sphere and a planar surface: Generalization of point-charge/surface image interaction to particle/surface image interaction // J. Colloid Interface Sci. – 1998. – V. 198, N 1. – P. 42–52.
42. *Lindell I.V., Dassios G., Nikoskinen K.I.* Electrostatic image theory for the conducting prolate spheroid // J. Phys. D: Applied Physics. – 2001. – V. 34, N 15. – P. 2302–2307.
43. *Messina R.* Image charges in spherical geometry: Application to colloidal systems // J. Chem. Phys. – 2002. – V. 117, N 24. – P. 11062–11074.
44. *Curtis R.A., Lue L.* Electrolytes at spherical dielectric interfaces // J. Chem. Phys. – 2005. – V. 123, N 17. – 174702/1–11.
45. *Gumbs G., Balassis A., Fekete P.* Image potential for a double-walled cylindrical nanotube // Phys. Rev. B. – 2006. – V. 73, N 7. – 075411/1–7.
46. *Messina R.* Electrostatics in soft matter // J. Phys. Condens. Matter. – 2009. – V. 21, N 11. – 113102/1–18.
47. *Antoniewicz P.R.* Effective polarizability of a point dipole near a metal surface with a Thomas-Fermi response // J. Chem. Phys. – 1972. – V. 56, N 4. – P. 1711–1714.
48. *Heinrichs J.* Response of metal surfaces to static and moving point charges and to polarizable charge distributions // Phys. Rev. B. – 1973. – V. 8, N 4. – P. 1346–1364.
49. *Kohn W., Lau K-H.* Adatom dipole moments on metals and their interactions // Solid State Commun. – 1976. – V. 18, N 5. – P. 553–555.
50. *Fuchs R., Barrera R.G.* Dynamical response of a dipole near the surface of a nonlocal metal // Phys. Rev. B. – 1981. – V. 24, N 6. – P. 2940–2950.
51. *Badiali J.P.* Structure of a polar fluid near a wall. Exact asymptotic behavior of the profile, relation with the electrostriction phenomena and the Kerr effect // J. Chem. Phys. – 1989. – V. 90, N 8. – P. 4401–4412.
52. *Villó-Pérez I., Abril I., Garcia-Molina R., Arista N.R.* Dynamical interaction effects on an electric dipole moving parallel to a flat solid surface // Phys. Rev. A. – 2005. – V. 71, N 5. – 052902/1–10.
53. *Barash Yu.S.* Van der Waals Forces. – M.: Nauka, 1988. – 344 p. (in Russian).
54. *Liang Y., Hilal N., Langston P., Starov V.* Interaction forces between colloidal particles in liquid: Theory and experiment // Adv. Colloid Interface Sci. – 2007. – V. 134–135. – P. 151–166.
55. *Scheel S., Buhmann S.Y.* Macroscopic quantum electrodynamics: concepts and applications // Acta Phys. Slovaca. – 2008. – V. 58, N 5. – P. 675–809.
56. *Giessibl F.J.* Advances in atomic force microscopy // Rev. Mod. Phys. – 2003. – V. 75, N 3. – P. 949–983.

57. *Giessibl F.J., Quate C.F.* Exploring the nanoworld with atomic force microscopy // Physics Today. – 2006. – V. 59, N 12. – P. 44–50.
58. *van de Leemput L.E.C., van Kempen H.* Scanning tunnelling microscopy // Rep. Prog. Phys. – 1992. – V. 55, N 8. – P. 1165–1240.
59. *Blanco J.M., Flores F., Pérez R.* STM-theory: Image potential, chemistry and surface relaxation // Prog. Surf. Sci. – 2006. – V. 81, N 10–12. – P. 403–443.
60. *Heinrichs J.* Response of metal surfaces to static and moving point charges and to polarizable charge distributions // Phys. Rev. B. – 1973. – V. 8, N 4. – P. 1346–1364.
61. *Gabovich A.M., Rozenbaum V.M., Voitenko A.I.* Dynamical image forces in three-layer systems and field emission // Surf. Sci. – 1987. – V. 186, N 3. – P. 523–549.
62. Voitenko A.I., Gabovich A.M. Dynamical image forces near the interface semiconductor-vacuum: the role of quantum-mechanical corrections // Fizika Tverdogo Tela. – 2001. – V. 43, N 12. – P. 2230–2236.
63. *Hou L.J., Mišković Z.L.* Image force on a charged projectile moving over a two-dimensional strongly coupled Yukawa system // Phys. Rev. E. – 2008. – V. 77, N 4. – 046401/1–7.
64. *Gabovich A.M., Il'chenko L.G., Pashitskii E.A., Romanov Yu.A.* Electrostatic energy and screened charge interaction near the surface of metals with different Fermi surface shape // Surf. Sci. – 1980. – V. 94, N 1. – P. 179–203.
65. *Somorjai G.A., Park J.G.* Frontiers of surface science // Physics Today. – 2007. – V. 60, N 10. – P. 48–53.
66. *Hotzel A., Moos G., Ishioka K.* et al. Femtosecond electron dynamics at adsorbate–metal interfaces and the dielectric continuum model // Appl. Phys. B. – 1998. – V. 68, N 3. – P. 615–622.
67. *Somorjai G.A., Park J.G.* Concepts, instruments, and model systems that enabled the rapid evolution of surface science // Surf. Sci. – 2009. – V. 603, N 10-12. – P. 1293–1300.
68. *Jackson J.D.* Classical Electrodynamics. – N.-Y.: John Wiley & Sons, 1998. – 808 p.
69. *Harrison W.A.* Solid State Theory. – N.-Y.: McGraw-Hill, 1970. – 572 p.
70. *Harned H.S., Owen B.B.* The Physical Chemistry of Electrolytic Solutions. – N.-Y.: Reinhold, 1950. – 547 p.
71. *Purcell E.M.* Electricity and Magnetism. Berkeley Physics Course. V. 2. – N.-Y.: McGraw-Hill, 1965. – 512 p.
72. *Tamm I.E.* Foundations of Electricity Theory. – M.: Nauka, 1976. – 616 p. (in Russian).
73. *Sivukhin D.V.* General Course of Physics. V. III. Electricity. Part 1. – M.: Fizmatlit, 1996. – 320 p. (in Russian).
74. *Gabovich A.M., Reznikov Yu.A., Voitenko A.I.* Excess nonspecific Coulomb ion adsorption at the metal electrode/electrolyte solution interface: Role of the surface layer // Phys. Rev. E. – 2006. – V. 73, N 2. – 021606/1–12.
75. *Simmons J.G.* Generalized formula for the electric tunnel effect between similar electrodes separated by a thin insulating film // J. Appl. Phys. – 1963. – V. 34, N 6. – P. 1793–1803.
76. *Gomer R., Swanson L.W.* Theory of field desorption // J. Chem. Phys. – 1963. – V. 38, N 7. – P. 1613–1629.
77. *Sidyakin A.V.* Calculation of the polarization contribution to the energy of the charge interaction with a metal surface. // JETP [Zhurn. Eksperim. Teoret. Fiz.]. – 1970. – V. 58, N 2. – P. 573–581.
78. *Partenskiĭ M.B.* Self-consistent electron theory of a metallic surface // Soviet Physics Uspekhi. – 1979. – V. 22, N 5. – P. 330–351.
79. *Kirzhnits D.A., Lozovik Yu.E., Shpatakovskaya G.V.* Statistical model of matter // Soviet Physics Uspekhi. – 1975. – V. 18, N 9. – P. 649–672
80. *Lindhard J.* On the properties of a gas of charged particles // Det Kongelige Danske Videnskabernes Selskab. Matematisk-fysiske Meddelelser. – 1954. – V. 28, N 8. – P. 1–57.
81. *Inkson J.C.* The electrostatic image potential in metal-semiconductor junctions / J. Phys. C: Solid State. – 1971. – V. 4, N 5. – P. 591–597.
82. *Schulze K-R., Unger K.* The linear dielectric response of a semiconductor: a new analytic form for the dielectric function // Phys. Status Solidi B. – 1974. – V. 66, N 2. – P. 491–498.
83. *Gabovich A.M., Voitenko A.I.* Influence of semiconductor dielectric function spatial dispersion on charge electrostatic energy near the semiconductor/vacuum interface and field emission current // Phys. Status Solidi B. – 1982. – V. 110, N 2. – P. 407–416.

84. *Gabovich A.M., Voitenko A.I.* Surface tension at the electrolyte solution/metal electrode interface. - II. The spatial dispersion of polar solvent dielectric permittivity // Electrochim. Acta. – 1986. – V. 31, N 7. – P. 777–782.
85. *Lang N.D.* The density-functional formalism and the electronic structure of metal surfaces // Solid State Phys. – 1973. – V. 28. – P. 225–300.
86. *Tung R.T.* Recent advances in Schottky barrier concepts // Mater. Sci. Eng. R. – 2001. – V. 35, N 1-3. – P. 1–138.
87. *Shpak A.P., Pogosov V.V., Kunitsky Yu.A.* Introduction to Physics of Ultradispersed Media. – K.: Akademperiodika, 2006. – 424 p. (in Russian).
88. *Singwi K.S., Tosi M.P.* Correlations in electronic liquids // Solid State Phys. – 1981. – V. 36. – P. 177–266.
89. *Lang N.D., Kohn W.* Theory of metal surfaces: charge density and surface energy // Phys. Rev. B. – 1970. – V. 1, N 12. – P. 4555–4568.
90. *Mahan G.D.* Many-Particle Physics. / 3rd Ed. – N.-Y.: Kluwer Academic, 2000. – 785 p.
91. *Inkson J.C.* The electron-electron interaction near an interface // Surf. Sci. – 1971. – V. 28, N 1. – P. 69–76.
92. *Inkson J.C.* Many-body effects at metal-semiconductor junctions. I. Surface plasmons and the electron-electron screened interaction // J. Phys. C: Solid State. – 1972. – V. 5, N 18. – P. 2599–2610.
93. *Lucas A.A.* Ion energy distributions in field-ion microscopy // Phys. Rev. B. – 1971. – V. 4, N 9. – P. 2939–2949.
94. *Inkson J.C.* The effective exchange and correlation potential for metal surfaces // J. Phys. F: Met. Phys. – 1973. – V. 3, N 12. – P. 2143–2156.
95. *Ray R., Mahan G.D.* Dynamical image charge theory // Phys. Lett. A. – 1972. – V. 42, N 4. – P. 301–302.
96. Šunjić M., Toulouse G., Lucas A.A. Dynamical corrections to the image potential. // Solid State Commun. – 1972. – V. 11, N 12. – P. 1629–1631.
97. *Chan D., Richmond P.* Classical theory of dynamical image interactions // Surf. Sci. – 1973. – V. 39, N 2. – P. 437–440.
98. *Sidyakin A.V.* Calculation of the polarization contribution to the energy of the charge interaction with a metal surface. // Phys. Solid State [Fiz. Tverdogo Tela]. – 1983. – V. 25. N 6. – P. 1885–1887 (in Russian).
99. *Hartstein A., Weinberg Z.A., DiMaria D.J.* Experimental test of the quantum-mechanical image-force theory // Phys. Rev. B. – 1982. – V. 25, N 12. – P. 7174–7182.
100. Stoneham A.M., Tasker P.W. Metal-nonmetal and other interfaces: the role of image interactions // J. Phys. C: Solid State. – 1985. – V. 18, N 19. – P. L543–L548.
101. *Alonso M., Alguacil F.J., Santos J.P. et al.* Deposition of ultrafine aerosol particles on wire screens by simultaneous diffusion and image force // J. Aerosol Sci. – 2007. – V. 38, N 12. – P. 1230–1239.

Received 02.02.2010, accepted 22.02.2010.

Дзеркальні сили у фізиці та хімії поверхні: деякі основні аспекти

О.М. Габович

Інститут фізики Національної академії наук України,
проспект Науки 46, Київ 03680, Україна

Аналізуються використання та роль дзеркальних у фізиці та хімії поверхні. Показано, що, на перший погляд, проста концепція класичної електростатики має непросте підґрунтя, пов'язане із розмаїтими багаточастинковими ефектами. Зокрема, звернено увагу на динамічні аспекти, зазвичай малі, проте важливі через свої особливі прояви.

Силы изображения в физике и химии поверхности: некоторые основные аспекты

А.М. Габович

Институт физики Национальной академии наук Украины,
проспект Науки 46, Киев 03680, Украина

Анализируются использование и роль сил изображения в физике и химии поверхности. Показано, что, на первый взгляд, простая концепция классической электростатики имеет сложную подоплёку, связанную с разнообразными многочастичными эффектами. В частности, привлекается внимание к динамическим аспектам, обычно малым, но, тем не менее, важным из-за своих особенных проявлений.